Extraction of the resonance parameters at finite times[*]

Ulf-G. Meißner[1,2],[†] Kathryn Polejaeva[1],[‡] and Akaki Rusetsky[1][§]

[1]*Helmholtz-Institut für Strahlen- und Kernphysik (Theorie),
and Bethe Center for Theoretical Physics,
Universität Bonn, 53115 Bonn, Germany and*

[2]*Forschungszentrum Jülich, Institut für Kernphysik (Theorie),
Jülich Center for Hadron Physics and Institute for
Advanced Simulation (IAS-4), D-52425 Jülich, Germany*

(Dated: July 7, 2010)

Abstract

In this paper we propose a model-independent method to extract the resonance parameters on the lattice directly from the Euclidean 2-point correlation functions of the field operators at finite times. The method is tested in case of the two-point function of the Δ-resonance, calculated at one loop in Small Scale Expansion. Further, the method is applied to a $1 + 1$-dimensional model with two coupled Ising spins and the results are compared with earlier ones obtained by using Lüscher's approach.

[†]Electronic address: meissner@hiskp.uni-bonn.de
[‡]Electronic address: polejaeva@hiskp.uni-bonn.de
[§]Electronic address: rusetsky@hiskp.uni-bonn.de

I. INTRODUCTION

It is well known that the asymptotic behavior of the two-point function for large Euclidean times is determined by the lowest eigenvalue of the Hamiltonian in a given channel. In case of stable particles, this property allows one to determine their masses. The case of the excited states is different. Here, the two-point function yields the spectrum of the so-called "scattering states." The relation to the energy and width of the resonance states is not direct, since a resonance, in general, can not be associated with an isolated energy level of a Hamiltonian. Up to now, several alternative methods have been used to determine these quantities from the lattice Monte Carlo (MC) simulations. These are:

i) At present, Lüscher's approach [1–4] is widely used to deal with the resonances in lattice QCD, obtained in simulations with sufficiently low quark masses. In brief, the procedure consists in determining first the phase shift by studying the volume dependence of the energy spectrum on the lattice. Then, continuing the S-matrix into the complex plane (e.g., by using the effective-range expansion whenever possible), one attempts to determine the position of the poles on the second Riemann sheet. This procedure is described in detail in Ref. [5], where the generalization to the case of the resonance matrix elements (in 1+1 dimensions) is also considered. A shortcut is provided by using Breit-Wigner type parameterization for the scattering phase and determining its parameters (energy and width) from the lattice data (see, e.g. Ref. [6] and Refs. [7, 8], where the method has been applied in the case of the σ- and ρ-mesons, respectively). The Lüscher's approach has been also generalized for the moving frames [9].

ii) Recently, the spectral functions in QCD have been reconstructed by using the maximal entropy method (see, e.g. [10–12]). This method, as well as Lüscher's approach, has in principle the capacity to address the problem of the extraction of the resonance energy and width from the Euclidean MC simulations on the lattice.

iii) The Euclidean correlators have been parameterized in terms of the energy and width of an isolated resonance state, in order to subsequently determine these quantities from the fit to the lattice data [13]. In that paper, the method has been applied to study the glueball decay.

iv) In certain cases, the decay width of an excited state can be evaluated by calculating decay amplitudes on the lattice (see, e.g. [14, 15]).

v) Recently, there has been a substantial activity in the determination of the excited meson and baryon spectrum by using generalized eigenvalue equations [16–23]. Despite spectacular progress achieved in the field, it should be stressed once again that a resonance state can not be uniquely associated with a particular energy level. To a certain extent, excited states and scattering states can be distinguished, e.g., by studying the volume dependence of the spectral density [24, 25]. This method, however works for narrow resonances only [26].

In this paper, we combine some of the above ideas and propose a systematic method to extract resonance pole positions from lattice data. In its present form, our approach is applicable to the systems with a low-lying, well-isolated, narrow resonance in the spectrum
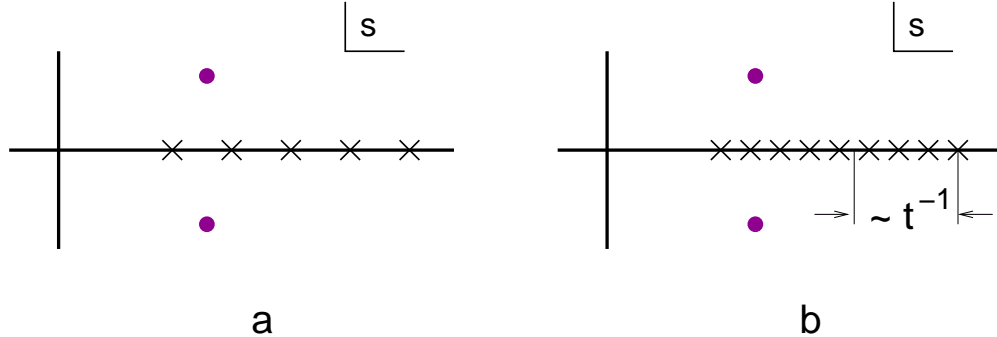
FIG. 1: Schematic representation of the analytic structure of the momentum-space two-point function in the rest frame $p_\mu = (\omega, 0)$ as a function of the complex variable $s = (i\omega)^2$, for two different values of the box size L. The crosses on the real axis denote the poles, and the shaded blobs, which are located symmetrically to the real axis, mark the location of the resonance poles on the second Riemann sheet emerging in the infinite volume limit. At any finite value of L, however, the two-point function is meromorphic and the second sheet does not arise. If the two-point function is measured for Euclidean times $\leq t$, the "energy resolution" of such a measurement is approximately equal to t^{-1}, as indicated on the right panel.

(for example, the ρ or the $\Delta(1232)$). First, we have tested our method using synthetic input data, represented by the Euclidean propagator of the Δ, calculated in the low energy effective field theory at one loop. A further test has been carried out in a 1+1 dimensional model of two coupled Ising spins, where the resonance parameters have been determined in the past utilizing Lüscher's approach [27, 28]. In both cases, we find that the method is capable to extract the pole position of the resonance.

The outline of the paper is as follows. In section II we discuss the foundations of the method. The general representation of the two-point function in the presence of a low-lying isolated resonance is discussed in section III. In section IV we consider the procedure of the data fitting and the determination of the pole position by using synthetic data. A short review of the 1+1 dimensional Ising model is given in section V. The extraction of the resonance pole in this model is considered in section VI. Finally, section VII contains our conclusions. Some technicalities are relegated to the appendices.

II.   KÄLLEN-LEHMANN REPRESENTATION

In the beginning of this section, we present a qualitative reasoning to justify our method. We start by mentioning that lattice QCD simulations are always carried out on lattices with a finite (Euclidean) time and spatial extension. Below, we consider lattices of the size $T \times L^d$, where T and L denote the box size in time and space, respectively, and d is the number of spatial dimensions. For not so large L (however, large enough to suppress the polarization effects in stable particles), the energy levels are well separated and can in principle be extracted from the asymptotic behavior of the two-point function at large Euclidean times $t \gg \Delta E$, where ΔE denotes the average level spacing. The Fourier-transform of the two-point function is a meromorphic function in the complex s-plane (see Fig. 1a). Consequently, the second Riemann sheet, as well as the poles on it (corresponding to the resonances), do not

appear at any finite L. The information about these poles stays encoded in the dependence of the spectrum on the spatial box size L and can be extracted (in several consecutive steps, as explained in the introduction) by using Lüscher's approach.

In case an almost stable state is present, such a complicated procedure might seem superfluous. Intuitively, it is clear that, if the decay width Γ is small, the resonance will behave pretty much the same way as a stable particle and will determine the t-dependence of the two-point function in a large interval (however, not for the asymptotically large times $t \gg \Gamma^{-1}$, when the resonance already has decayed). Consider, for example, a lattice with the large spatial size L, and calculate the two-point function at finite t (see Fig. 1b). If the "resolution" $\sim t^{-1}$ is larger than the distance between energy levels, the two-point function is given by a sum of (many) exponentials with the spectral weight suppressed by a factor L^{-d}, so that, effectively, the spectral sum transforms into an integral over the energies. This is equivalent to the emergence of the cut that connects the physical sheet to the second sheet. We expect that, in this case, one may find an alternative representation of the two-point function in terms of *quasiparticle* degrees of freedom corresponding to the pole(s) on the second Riemann sheet (i.e. the resonance decay and width) plus a small background which can be described by a few parameters. Namely, we expect that there exists a window in the variable t, where such a description will be more effective than the multi-exponential representation through the energies and spectral weights.

Hence, the original problem is reduced to finding a universal, model-independent parameterization of the two-point function in the presence of a narrow resonance, which will allow one to determine the energy and the width of the latter by performing a fit to the lattice data. This is analogous to the exponential parameterization, which allows one to determine the mass of a stable particle by fitting at asymptotically large times. Note that we shall try to avoid approximations in the spectral function (e.g. the narrow width approximation used in Ref. [13]), which are a potential source of a systematic error. The contribution of the background, albeit small, will be taken into account in a systematic manner.

The model-independent parameterization, which was mentioned above, can be obtained directly by using the Källen-Lehmann representation for the two-point function. Below, we give a brief derivation of this representation in a finite box. Further, we consider the limits $T \to \infty$ and $L \to \infty$ in detail, in order to quantify the qualitative arguments given in the beginning of this section.

In the derivation of the Källen-Lehmann representation in a finite volume, we mainly follow the steps given in Ref. [10]. Let $\phi(x) \doteq \phi(t, \mathbf{x})$ be any local field, carrying the resonance quantum numbers. The two-point function of this field in the Euclidean space is defined as

$$D(t,\mathbf{x}) = \langle N_t [\phi(t,\mathbf{x})\phi^\dagger(0)]\rangle = \frac{1}{Z(T)} \mathrm{Tr}\left(N_t [\phi(t,\mathbf{x})\phi^\dagger(0)]\,\mathrm{e}^{-HT}\right),$$

$$N_t [\phi(t,\mathbf{x})\phi^\dagger(0)] \doteq \theta(t)\phi(t,\mathbf{x})\phi^\dagger(0) \pm \theta(-t)\phi^\dagger(0)\phi(t,\mathbf{x}),$$

$$Z(T) = \mathrm{Tr}\left(\mathrm{e}^{-HT}\right), \tag{1}$$

where the upper (lower) sign corresponds to bosons (fermions). The Fourier transform of this expression takes the form

$$D(t,\mathbf{x}) = \frac{1}{TL^d} \sum_\omega \sum_\mathbf{k} D(i\omega,\mathbf{k})\,\mathrm{e}^{-i\omega t - i\mathbf{k}\mathbf{x}}, \tag{2}$$

4

where $\omega = \frac{2\pi}{T} n_T$ $\left(\omega = \frac{\pi}{T}(2n_T + 1)\right)$, with $n_T \in \mathbb{Z}$, are Matsubara frequencies in case of bosons (fermions), and $\mathbf{k} = \frac{2\pi}{L} \mathbf{n}$ with $\mathbf{n} \in \mathbb{Z}^d$.

Using a complete set of Hamiltonian eigenvectors $H|\alpha\rangle = E_\alpha |\alpha\rangle$ to calculate the trace in Eq. (1), one gets

$$D(i\omega, \mathbf{k}) = -\frac{L^d}{Z(T)} \sum_\alpha \sum_\beta \delta^d_{\mathbf{k}, \mathbf{p}_\beta - \mathbf{p}_\alpha} \frac{\mathrm{e}^{-E_\alpha T} \mp \mathrm{e}^{-E_\beta T}}{E_\alpha - E_\beta + i\omega} \langle\alpha|\phi(0)|\beta\rangle \langle\beta|\phi^\dagger(0)|\alpha\rangle, \tag{3}$$

where $\delta^d_{\mathbf{k}, \mathbf{q}}$ denotes the periodic Kronecker δ in d dimensions. This relation can be rewritten as

$$D(i\omega, \mathbf{k}) = \int_{-\infty}^{\infty} \frac{d\omega'}{\omega' - i\omega} A(\omega', \mathbf{k}), \tag{4}$$

where the spectral function is given by

$$A(\omega', \mathbf{k}) = \frac{L^d}{Z(T)} \sum_\alpha \sum_\beta (\mathrm{e}^{-E_\alpha T} \mp \mathrm{e}^{-E_\beta T}) \, \delta(\omega' - E_\beta + E_\alpha) \, \delta^d_{\mathbf{k}, \mathbf{p}_\beta - \mathbf{p}_\alpha} \langle\alpha|\phi(0)|\beta\rangle \langle\beta|\phi^\dagger(0)|\alpha\rangle. \tag{5}$$

By applying discrete symmetries, it can be shown that the spectral function obeys the following properties [10]

$$A(\omega', \mathbf{k}) \geq 0 \quad \text{for} \quad \omega' \geq 0, \qquad A(-\omega', -\mathbf{k}) = \mp A(\omega', \mathbf{k}) = \mp A(\omega', -\mathbf{k}). \tag{6}$$

The dispersion integral can be rewritten as[1]

$$D(i\omega, \mathbf{k}) = \int_0^\infty \frac{d\omega'^2}{\omega'^2 + \omega^2} A(\omega', \mathbf{k}). \tag{7}$$

Finally, in the limit $T \to \infty$, only the vacuum state $\alpha = 0$, $E_\alpha = 0$ contributes, and the spectral function in Eq. (7) is given by

$$\lim_{T \to \infty} A(\omega', \mathbf{k}) = L^d \sum_\beta \delta(\omega' - E_\beta) \, \delta^d_{\mathbf{k}, \mathbf{p}_\beta} \, |\langle 0|\phi(0)|\beta\rangle|^2. \tag{8}$$

Now, let the variable ω^2 be outside the narrow strip along the negative real axis. Then, the function $2\omega'(\omega'^2 + \omega^2)^{-1}$ for all $0 \leq \omega' < \infty$ is uniformly bound from above by some large constant B. For fixed B, performing the limit $L \to \infty$ and applying the regular summation theorem [29], it is seen[2] that the quantity $D(i\omega, \mathbf{k})$ approaches $D^\infty(i\omega, \mathbf{k})$, with the pertinent spectral function given by

$$A^\infty(\omega', \mathbf{k}) = \sum_\beta \delta(\omega' - E_\beta) \, (2\pi)^d \delta^d(\mathbf{k} - \mathbf{p}_\beta) \, |\langle 0|\phi(0)|\beta\rangle|^2, \tag{9}$$

---

[1] For illustrative purpose, below we display the bosonic case only. The fermionic case can be treated similarly.

[2] The regular summation theorem implies that the matrix elements $\langle 0|\phi(0)|\beta\rangle$ are continuous functions of E_β. We examine these matrix elements explicitly in a simple quantum mechanical model in Appendix A and show that in this case the above requirement is indeed fulfilled.

where $\sum_\beta$ stands for the sum (integral) over the continuous spectrum wave functions. More precisely, for ω^2 outside the strip

$$|D(i\omega, \mathbf{k}) - D^\infty(i\omega, \mathbf{k})| \leq B \int_{\omega_{\mathsf{min}}}^\infty d\omega' |A(\omega', \mathbf{k}) - A^\infty(\omega', \mathbf{k})|, \tag{10}$$

where ω_{min} is determined by the invariant mass of the lowest-mass state. Further, according to the regular summation theorem, the difference $A(\omega_0, \Delta, \mathbf{k}) - A^\infty(\omega_0, \Delta, \mathbf{k})$, where

$$A(\omega_0, \Delta, \mathbf{k}) = \int_{\omega_0 - \Delta/2}^{\omega_0 + \Delta/2} d\omega' A(\omega', \mathbf{k}), \qquad A^\infty(\omega_0, \Delta, \mathbf{k}) = \int_{\omega_0 - \Delta/2}^{\omega_0 + \Delta/2} d\omega' A^\infty(\omega', \mathbf{k}), \tag{11}$$

for any $\omega_0 > \omega_{\mathsf{min}}$ and $\Delta > 0$ converges faster than any power of L as $L \to \infty$ (for a discussion, see Appendix A). In other words, in this limit the two-point function converges to its infinite-volume counterpart everywhere in the complex plane except the narrow strip along the cut (for a related discussion, see also Ref. [30]). This statement is a mathematical formulation for the intuitive picture of "poles merging into the cut," which is shown in Fig. 1b. To further illustrate this, an example of a function which is meromorphic at a finite L and develops a cut and a pole on the second Riemann sheet in the limit $L \to \infty$, is given in Appendix B.

Moreover, from Eq. (2) one finds

$$D(t, \mathbf{k}) = \frac{1}{T} \sum_\omega \mathrm{e}^{-i\omega t} D(i\omega, \mathbf{k}) = \int_{\omega_{\mathsf{min}}}^\infty d\omega' \frac{\mathrm{e}^{-\omega'(T-t)} + \mathrm{e}^{-\omega' t}}{1 - \mathrm{e}^{-\omega' T}} A(\omega', \mathbf{k})$$

$$\to \int_{\omega_{\mathsf{min}}}^\infty d\omega' \mathrm{e}^{-\omega' t} A(\omega', \mathbf{k}). \tag{12}$$

The last line is obtained in the limit $T \to \infty$. Together with the expression (8) for the spectral density, we recover the representation for $D(t, \mathbf{k})$ as a sum over exponentials. In the case t^{-1} is much larger than the distance between different energy levels (this can be achieved, e.g., by holding t fixed and increasing L), many exponentials contribute to $D(t, \mathbf{k})$ and the sum over the energy eigenvalues can be replaced through the integral. In this case, $A(\omega', \mathbf{k})$ is replaced by $A^\infty(\omega', \mathbf{k})$.

To summarize, the behavior of the two-point function can be studied in different regimes. For asymptotically large t and moderately large L, only the few lowest, well-separated energy levels contribute. This situation is well described by a sum of a few exponential terms. In difference to this, in the regime with asymptotically large L and moderately large t there are many terms with nearly the same energies that contribute to the multi-exponential representation. The sum over the discrete energy spectrum effectively transforms into an integral. If, in addition, a low-lying well separated resonance emerges, we expect that the spectral integral can be efficiently parameterized in terms of the resonance parameters instead of the stable energy levels.

III.   TWO-POINT FUNCTION AT FINITE t

As discussed in the previous section, it is possible to perform the infinite-volume limit $L \to \infty$ in the two-point function, keeping the Euclidean time t fixed. The spectral representation

is given by Eq. (7) with the spectral density given by Eq. (9). Note that the spectral density vanishes for $0 \leq \omega' \leq w_{\mathsf{min}}$, and hence the integration in Eq. (7) in fact is performed from $\omega'^2 = \omega_{\mathsf{min}}^2$ to infinity.

For simplicity, we work in the center-of-mass (CM) frame $\mathbf{k} = 0$ and denote $D(i\omega, \mathbf{0}) \doteq D(i\omega)$, $A^\infty(\omega', \mathbf{0}) \doteq A(\omega')$. The spectral representation then takes the form

$$D(i\omega) = \int_{\omega_{\mathsf{min}}}^\infty \frac{2\omega' d\omega'}{\omega'^2 + \omega^2} A(\omega') . \tag{13}$$

In the vicinity of the elastic threshold, $A(\omega') \sim (\omega' - \omega_{\mathsf{min}})^{l+1/2}$, where l stands for the orbital angular momentum[3].

Assume now that an isolated low-lying resonance emerges. This is equivalent to the statement that the function $A(\omega')$ takes the form

$$A(\omega') = \frac{(\omega' - \omega_{\mathsf{min}})^{l+1/2}}{(\omega' - \omega_R)(\omega' - \omega_R^*)} Q(\omega') , \tag{14}$$

where the singularities of the function $Q(\omega')$ lie far enough from the threshold so that the Taylor expansion of this function converges in the part of the complex plane that includes the resonance poles at $\omega' = \omega_R$ and $\omega' = \omega_R^*$. The energy and the width of the resonance is determined by ω_R in the standard manner. Note that these poles come in complex-conjugated pairs[4].

Using Eq. (14), it can be easily shown that

$$D(t) = \int_{\omega_{\mathsf{min}}}^\infty d\omega' \, \mathrm{e}^{-\omega' t} A(\omega') = \mathrm{e}^{-\omega_{\mathsf{min}} t} \int_0^\infty \frac{dE E^{l+1/2} \mathrm{e}^{-Et}}{(E - E_R)(E - E_R^*)} Q(E + \omega_{\mathsf{min}}) , \tag{15}$$

where $E_R = \omega_R - \omega_{\mathsf{min}} = E_0 - i\Gamma/2$. As mentioned before, it is assumed that the Taylor expansion $Q(E + \omega_{\mathsf{min}}) = \sum_{k=0}^\infty q_k E^k$ converges in the part of a complex region which includes the resonance poles.

From the above expression we get

$$D(t) = \mathrm{e}^{-\omega_{\mathsf{min}} t} \sum_{k=0}^\infty q_k F^{(k+l)}(t, E_R) , \qquad F^{(m)}(t, E_R) = \int_0^\infty \frac{dE E^{m+1/2} \mathrm{e}^{-Et}}{(E - E_0)^2 + \Gamma^2/4} . \tag{16}$$

In particular, for $m = 0, 1$, we find

$$F^{(0)}(t, E_R) = -\frac{2}{\Gamma} \operatorname{Im} \chi(t, E_R)$$

$$F^{(1)}(t, E_R) = \operatorname{Re} \chi(t, E_R) - \frac{2E_0}{\Gamma} \operatorname{Im} \chi(t, E_R), \tag{17}$$

where

$$\chi(t, E_R) = \int_0^\infty \frac{dE \, E^{1/2} \mathrm{e}^{-Et}}{E - E_R} \tag{18}$$

---

[3] This statement is valid in 3+1 dimensions. In 1+1 dimensions, one has to substitute $l = 0$ in all formulae.

[4] $A(\omega')$ is the discontinuity of a function which is analytic in the cut complex plane and obeys Schwarz reflection principle. Hence the poles in this function (which emerge on the second Riemann sheet), always come in pairs. This is the justification for the ansatz (14).
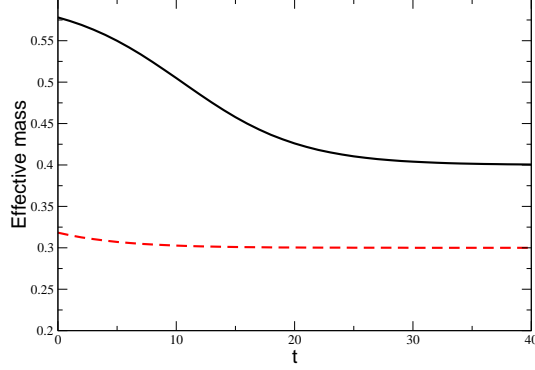
FIG. 2: Schematic representation of the effective mass for a stable particle (dashed line) and for a resonance (solid line).

and the following representation in form of an infinite series is useful in a wide range of the variable t

$$\chi(t, E_R) = -\pi \sqrt{-E_R}\, e^{-E_R t} + \sqrt{\frac{\pi}{t}} \left\{ 1 + \sum_{k=0}^{\infty} \frac{(-2E_R t)^{k+1}}{(2k+1)!!} \right\}. \tag{19}$$

Further, the functions $F^{(m)}$ with $m \geq 2$ can be recursively expressed through $F^{(0,1)}$. The general representation of the two-point function follows straightforwardly from the above relations

$$D(t) = e^{-\omega_{\min} t} \left\{ c_0 F^{(0)}(t, E_R) + c_1 F^{(1)}(t, E_R) + \sum_{k=0}^{\infty} \frac{x_k}{t^{l+k+3/2}} \right\}, \tag{20}$$

where $c_{0,1}$ and x_k are expressed through the Taylor coefficients q_k as well as E_0, Γ.

Eq. (20) represents our central result. It provides a universal parameterization of the Euclidean two-point function in the presence of a low-lying isolated resonance described by two parameters E_0, Γ. The couplings x_k are associated with the non-resonant background. In particular, it encodes the contribution of the threshold which lies *below* the resonance energy. This means that if t is taken too large, the background dominates and the information about E_0, Γ is erased. We assume, however, that in the presence of a narrow resonance, there exists a sufficiently wide window in t, where the background is small and E_0, Γ can be determined from the fit of the measured $D(t)$ to the representation (20). We require that, in this window, adding the background parameterized by the constants x_k should lead to small corrections in E_0, Γ and the fit should remain stable against the increase of the number of independent x_k.

The physical meaning of our method can be easily illustrated by Fig. 2. In this figure, the effective mass of a system in the presence of a stable state/resonance is schematically depicted. If there is a stable particle, the plateau in the effective mass sets in almost immediately. However, if a resonance instead of a stable particle is present, there exists a wide window in t, where many excited states contribute and the effective mass decreases slowly until it reaches the asymptotic value. Our method roughly corresponds to fitting $D(t)$ within this interval by the representation given in Eq. (20), and the decay width is determined by the rate of the decrease of the effective mass. Note that a similar picture was obtained in Ref. [31]. In that paper, the theory of two coupled scalar fields, where the

8

heavier field can decay into a couple of light scalars, was considered. In particular, it has been shown that the effective mass of the heavy scalar, calculated on the lattice, exhibits the same behavior when its mass is below/above the two-particle threshold (see Fig. 1 of that article). The two point functions of the excited mesons in QCD also exhibit a similar behavior [16].

It is instructive to compare the parameterization (20) to the pertinent formula obtained in Ref. [13]. A technical difference consists in the absence of the threshold factor $(\omega' - \omega_{\mathsf{min}})^{l+1/2}$ that results in a different parameterization of the background. The important difference is, however, that in Ref. [13] a Breit-Wigner type parameterization for the spectral function is originally assumed. Since this ansatz did not fit the lattice data well, an *ad hoc* energy-dependence in the decay width has been introduced, and the functional form of this dependence has been determined by using a trial-and-error method. In our approach, the representation of $D(t)$, given in Eq. (20) is completely general and is based on the sole assumption that a well-isolated resonance emerges at low energies. The background is parameterized by the constants x_k in a systematic manner.

IV. THE FIT

We first test our method by using synthetic data. Consider, for instance, the propagator of the Δ-resonance evaluated in the Small Scale Expansion (SSE)[5] at one loop [33, 34]. In the Minkowski space, this propagator is given by

$$S_\Delta(p) = -S_\Delta^{3/2}(p)\Pi^{3/2} + \text{spin-}1/2\,,$$

$$S_\Delta^{3/2}(p) = \frac{1}{\mathring{m}_\Delta(1 + \Sigma_2(p^2)) - \not{p}(1 - \Sigma_1(p^2))}\,, \qquad (21)$$

where $\mathring{m}_\Delta$ denotes the mass of the Δ-resonance in the chiral limit, $\Pi^{3/2}$ stands for the projector onto the spin-3/2 state and the spin-1/2 part does not have a pole in the low-energy region (for a general proof of this statement, see [35]). Further, the invariant functions $\Sigma_{1,2}(p^2)$ at order p^3 in the chiral expansion are given by

$$\Sigma_1(s) = \frac{c_A^2}{F^2}\left(W_2(s) - W_3(s)\right)\,, \qquad \Sigma_2(s) = \frac{c_A^2}{F^2}\frac{m_N}{m_\Delta}W_2(s)\,, \qquad (22)$$

where c_A and F denote the $\pi N\Delta$ coupling constant and the pion decay constant in the chiral limit, respectively, m_N, m_Δ, M_π are the nucleon, Δ and pion masses, respectively, and the

---

[5] The SSE is a phenomenological extension of Chiral Perturbation Theory in which the Δ-nucleon mass splitting is counted as an additional small parameter. This quantity, however, does not vanish in the chiral limit. The framework of the SSE is laid in detail in Ref. [32].

invariant functions $W_{2,3}$ are given by [33, 34]

$$W_3(s) = \frac{-s + m_N^2 - M_\pi^2}{-2s} W_2(s) + \frac{M_\pi^4}{128\pi^2 s}\left(\ln\frac{M_\pi^2}{m_N^2} + \frac{1}{6}\right),$$

$$W_2(s) = -\frac{1}{12s}\left(\lambda W_0(s) - (-s + m_N^2 - M_\pi^2)\frac{M_\pi^2}{16\pi^2}\ln\frac{M_\pi^2}{m_N^2}\right),$$

$$W_0(s) = \frac{i\sqrt{\lambda}}{16\pi s} - \frac{s - m_N^2 + M_\pi^2}{32\pi^2 s}\left(\ln\frac{M_\pi^2}{m_N^2} - 1\right) - \frac{\sqrt{\lambda}}{32\pi^2 s}\ln\frac{s + M_\pi^2 - m_N^2 + \sqrt{\lambda}}{s + M_\pi^2 - m_N^2 - \sqrt{\lambda}},$$

$$\lambda = (s - (m_N + M_\pi)^2)(s - (m_N - M_\pi)^2). \tag{23}$$

The trace of $S_\Delta^{3/2}(p)$ obeys the dispersion relation

$$\text{Tr}\, S_\Delta^{3/2}(p) = \frac{4\mathring{m}_\Delta(1 + \Sigma_2(p^2))}{(\mathring{m}_\Delta(1 + \Sigma_2(p^2)))^2 - p^2(1 - \Sigma_1(p^2))^2} = \int_{(m_N + M_\pi)^2}^\infty \frac{ds'}{s' - p^2 - i\epsilon} A(s'), \tag{24}$$

where the expression for the discontinuity can be directly read off from Eqs. (21)-(23).

In the calculations we have used the following values of the parameters: $m_N = 940$ MeV, $M_\pi = 140$ MeV, $m_\Delta = \mathring{m}_\Delta = 1232$ MeV, $F = F_\pi = 92.4$ MeV and $c_A = 1.5$ (this value leads to the width $\Gamma = 124$ MeV in a $O(\epsilon^3)$ calculation at $p^2 = m_\Delta^2$). It is easy to check that the propagator has a pole at $m_R = 1212$ MeV and $\Gamma = 76$ MeV (note the large shift in the quantity Γ as compared to its value obtained at $p^2 = m_\Delta^2$ that presumably is an artefact of a $O(\epsilon^3)$ approximation).

Next, we wish to investigate whether it is possible to recover this result by applying our method. To this end, we analytically continue Eq. (24) into Euclidean space and perform the Fourier transform with respect to the fourth component of the momentum. The resulting values are treated as synthetic data. We choose the interval $1.7M_\pi^{-1} < t < 4M_\pi^{-1}$ and perform a least squares fit of these data to the formula (20) (the data points are assumed to be distributed equidistantly in this interval).

In the fit, we cut the sum in Eq. (20) at some value k_{max}. The fit of the 7 data points with $k_{\text{max}} = 0$ yields $m_R = 1213$ MeV and $\Gamma = 74$ MeV that is already close to the exact values. The procedure converges rapidly. At the accuracy of the digits displayed, the exact result is obtained for $k_{\text{max}} = 2$. Adding more terms, it is possible to improve the agreement with the exact result up to very many decimal digits.

To summarize, using synthetic data, we have demonstrated that our method is capable to reconstruct the exact position of a pole in a complex plane from a limited data sample. To perform a similar analysis for real Monte Carlo data is much more challenging. One of the main problems that we have encountered there, is related to the instability of the fit when k_{max} increases (this problem already arises for relatively small $k_{\text{max}} = 3$ or 4). Namely, the constants x_k, which describe the background, become very large in magnitude having alternating signs and this destabilizes the values of E_0, Γ extracted from the fit.

In order to circumvent this problem, we have performed a Bayesian fit to the lattice MC data. A detailed description of the Bayesian fit techniques, which is well suited for our purposes, can be found, e.g. in Ref. [36]. We shall present a brief summary of the method below. The function to be minimized in the standard least squares fit is given by

$$\chi^2 = \sum_i \left(D(t_i, E_0, \Gamma, c_1, c_2, x_k) - \bar{D}(t_i)\right)^2, \tag{25}$$

10

where $\bar{D}(t_i)$ are data corresponding to the points t_i. In Eq. (25) it is implicitly assumed that the MC errors in the data $\bar{D}(t_i)$ do not vary much with t_i. Note that the above form still does not include our prior knowledge about x_k. The assumption about the smoothness of the function $Q(\omega')$ in Eq. (14) implies that x_k should be of "natural size" excluding the scenario where the x_k become large with alternating signs.

In order to implement this prior knowledge into the fitting procedure, in analogy with Ref. [36], we define the augmented χ^2

$$\chi^2_{\text{aug}} = \chi^2 + \chi^2_{\text{prior}}, \qquad \chi^2_{\text{prior}} = \frac{1}{S^2} \sum_{k=0}^{k_{\text{max}}} x_k^2, \qquad (26)$$

where S is some scale that ensures that all x_k stay in the "natural" range.

We determine the quantity S by using the trial-and-error method. If S is too large, the introduction of χ^2_{aug} does not cure the problem with the convergence. This sets the upper limit on the value of S. The lower limit for S is set by the requirement that the results obtained with standard χ^2 and χ^2_{aug} agree for low $k_{\text{max}} = 1, 2$. In addition, within this range, the final result of the fit for E_0, Γ should not depend on S.

In the 1+1 dimensional model with two Ising spins discussed in the next section, we have performed fits using χ^2_{aug}. Below we show that this technique allows one to extract the precise values of E_0, Γ from the lattice MC data in this model.

V. 1 + 1 DIMENSIONAL MODEL WITH TWO COUPLED ISING SPINS

In this section we apply our method to the extraction of the resonance pole position to a 1+1 dimensional model of two coupled Ising spins. This model has been treated in Refs. [27, 28] using Lüscher's approach. In particular, it has been shown that a narrow resonance emerges in the system, whose parameters can be extracted in a systematic manner.

The action of the model is given by

$$S = -\kappa_\phi \sum_{z\in\Lambda,\hat{\mu}=1,2} \phi_z\,\phi_{z+\hat{\mu}} - \kappa_\eta \sum_{z\in\Lambda,\hat{\mu}=1,2} \eta_z\eta_{z+\hat{\mu}} + \frac{g}{2} \sum_{z\in\Lambda,\hat{\mu}=1,2} \eta_z\phi_z\,(\phi_{z-\hat{\mu}} + \phi_{z+\hat{\mu}}), \qquad (27)$$

where $\phi_z, \eta_z = \pm 1$ are two Ising spins which interact with each other through the Yukawa-type coupling $g\eta\phi\phi$. The sum $z \in \Lambda$, where $z = (x,t)$, runs over all lattice points and $\hat{\mu}$ denotes the unit vector along the spatial axis. The couplings $\kappa_\phi, \kappa_\eta > 0$ are chosen so that the masses of ϕ and η are $m_\phi \simeq 0.19$ and $m_\eta \simeq 0.5$ (in lattice units). Note that, if $g \neq 0$, the η decays into 2ϕ, so m_η corresponds to the resonance energy in this case.

The model has been analyzed in detail in Refs. [27, 28]. We give only a short summary of this analysis here. In particular, it has been argued that in the theory described by the Lagrangian (27) no second-order phase transition occurs and thus the continuum limit can not be performed. In other words, all results obtained here refer to the effective theory with an ultraviolet cutoff.

The energy spectrum is determined by solving the generalized eigenvalue problem. The operator basis is defined as in Refs. [27, 28]

$$\mathcal{O}_1(t) = \frac{1}{L} \sum_x \eta_{x,t}, \qquad \mathcal{O}_j(t) = \frac{1}{L^2} \sum_{xy} \phi_{x,t}\phi_{y,t}\mathrm{e}^{-ip_j(x-y)}, \qquad p_j = \frac{2\pi(j-2)}{L}, \qquad (28)$$
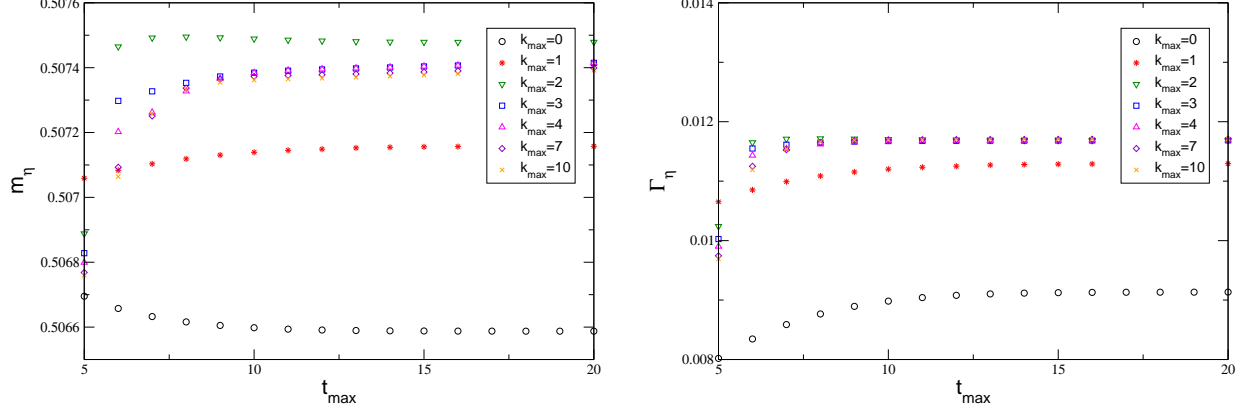
FIG. 3: Checking the convergence of m_η (left panel) and Γ_η (right panel) against the variation of t_{max} and k_{max}, for $L = 60$. A similar behavior is observed for smaller values of L.

with $j = 2, 3, \cdots$. The correlator matrix is given by

$$C_{ij}(t) = \langle \mathcal{O}_i(t)\mathcal{O}_j(0)\rangle - \langle \mathcal{O}_i(t)\rangle\langle \mathcal{O}_j(0)\rangle. \tag{29}$$

The spectral decomposition of $C_{ij}(t)$ is approximated by the truncated series

$$C_{ij}(t) = \sum_{l=1}^{r} v_i^{(l)} v_j^{(l)*} \, \mathrm{e}^{-W_l t}. \tag{30}$$

The energy eigenvalues W_l for $l = 1, \cdots, r$ are determined by diagonalizing the matrix $M(t, t_0) \doteq C^{-1/2}(t_0)C(t)C^{-1/2}(t_0)$, where t_0 is some fixed time (in the following, as in Refs. [27, 28], we always use $t_0 = 1$). The eigenvalue equation takes the form

$$M(t, t_0)u^{(l)} = \lambda^{(l)}(t, t_0)u^{(l)}, \qquad \lambda^{(l)}(t, t_0) = \mathrm{e}^{-W_l(t-t_0)}, \quad l = 1 \cdots r, \tag{31}$$

where $u^{(l)}$ form an orthonormal basis. The eigenvectors $v^{(l)}$ are given by $v^{(l)} = \exp(W_l t/2)\, C^{1/2}(t_0)u^{(l)}$.

The MC simulation is done by using a cluster algorithm [37]. We closely followed the procedure described in [27, 28] and, using the parameter set $\kappa_\phi = 0.3700$, $\kappa_\eta = 0.3700$, $g = 0.04$, have reproduced the L-dependent spectrum calculated in this paper. The resonance parameters found in Refs. [27, 28] are: $m_\eta = 0.5112(3)$ and $\Gamma_\eta = 0.0100(3)$. It remains to be seen, whether the same result can be obtained by using our approach.

VI.   RESULTS

In order to use our method, one has to calculate the two-point function within a sufficiently large interval in the Euclidean time t and then fit the result with Eq. (20). To this end, the correlator $C_{11}(t)$ has been chosen, see Eq. (29). However, as already mentioned in [27, 28], the simulations become unstable already at $t \simeq t_{\mathsf{unst}} = 5 - 8$, depending on the value of L chosen. The statistical error in the effective mass of η at $t > t_{\mathsf{unst}}$ blows up, rendering an accurate fit impossible. The use of improved estimators or a substantial increase of the number of configurations results only in a moderate improvement of the error in $C_{11}(t)$.

As described above, the energy spectrum of the system can be determined with high accuracy from the correlator matrix $C_{ij}(t)$ at $t \leq t_{\mathsf{unst}}$ by applying the generalized eigenvalue method. In addition to the ground state, the approach allows a reliable extraction of higher excited levels (up to 4 or 5 levels, depending on L). The physical reason for this is that the matrix $C_{ij}(t)$ contains much more information about the system than the single function $C_{11}(t)$. In particular, it contains information about the matrix elements describing the transitions between various energy levels.

So, it is not surprising that using this input in our method helps to reduce the errors dramatically and to stabilize the fit. In brief, the procedure can be described as follows:

1. The energy spectrum W_l and the wave functions $v^{(l)}$ are accurately determined by measuring the matrix $C_{ij}(t)$ at $t \leq t_{\mathsf{unst}}$. We choose $t_{\mathsf{unst}} = 5$ for all L and average all W_l for $t = t_0 \cdots (t_{\mathsf{unst}} - 1)$.

2. The function $C_{11}(t)$ is approximated by the multi-exponential function $C_{11}(t) = \sum_{l=1}^{r} z_l \exp(-W_l t)$, where the $z_l = |v_1^{(l)}|^2$ are averaged for all $t = t_0 \cdots (t_{\mathsf{unst}} - 1)$. This approximation is used for $t > t_{\mathsf{unst}}$ as well. Note that z_l, $l \neq 1$ encode the information about the overlap of η and 2ϕ states that determines the decay width of a resonance.

3. The expression (20) is fitted to the $C_{11}(t)$ which is approximated by the multi-exponential function.

The MC simulations were carried out for various lattice sizes in the interval $L = 24 - 60$, while the value $T = 100$ remained fixed throughout the simulations. We have used bases containing 4-6 operators and performed test runs for some (large) values of L by using the basis of 8 and 10 operators. In the fit, all data between $t = 1$ and $t = t_{\mathsf{max}}$ were used. The errors in our results are purely statistical and were estimated by performing 5 independent simulations with 10^6 configurations each. In addition, we find that the increase of the number of operators to 8 or 10 operators does not affect the result within the errors.

First, the stability of our results was checked, when t_{max} and k_{max} increase. The result of this check is displayed in Fig. 3, where the dependence of the real and imaginary parts of the resonance pole position on t_{max} is plotted for different values of k_{max}. It is seen that for $t_{\mathsf{max}} \geq 10 - 12$ both the energy and the width remain almost constant and converge rapidly in k_{max} already at $k_{\mathsf{max}} = 3$, if the Bayesian fit is performed. The similar behavior is observed at all values of L. The final result for the resonance pole parameters is always given at $k_{\mathsf{max}} = 10$.

In order to ensure that, performing the Bayesian fit, a bias is not introduced in the extracted values of the resonance parameters, one has to check that there exists a range of the scale parameter S where the energy and the width depend weakly on S. The results for both quantities at different values of L look qualitatively similar. In Fig. 4 we present the plot for the width at $L = 60$. As seen from Fig. 4, a wide plateau emerges around $S \simeq 10^5$, where the scale dependence practically disappears while the convergence in k_{max} still persists. This is the window, where the extraction of the width is finally carried out. Increasing S even further, the convergence in k_{max} breaks down, and the result can not be trusted any longer.

Finally, since our MC data have been calculated at a finite L, whereas the formula (20) refers to the limit $L \to \infty$, there is an expected residual volume dependence in the parameters E_0, Γ. The Fig. 5 displays this dependence. In particular, it is seen that there is a rather
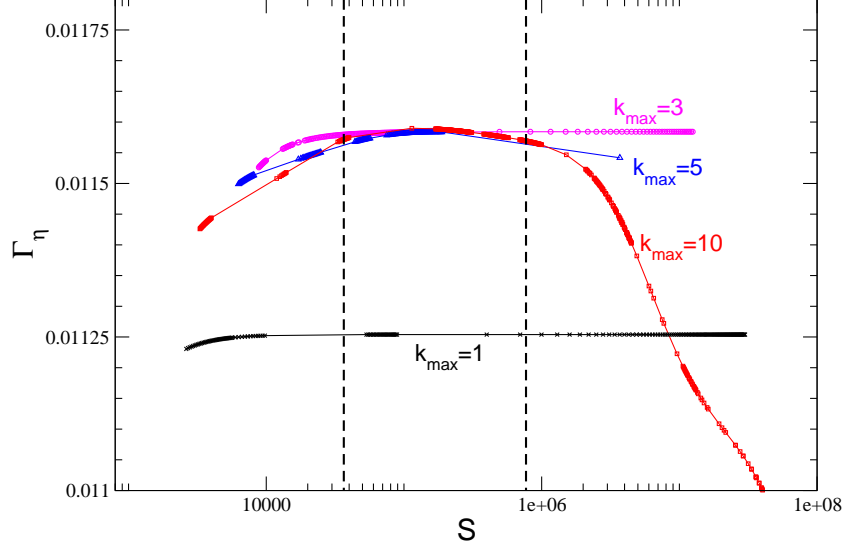
13

FIG. 4: Dependence of the width on the scale S used in the Bayesian fit at different k_{max}. For small values of S, the result is scale-dependent. For large S, the result does not converge with k_{max}. There exists a plateau around $S \simeq 10^5$ where the procedure converges and yields a scale-independent result.

strong variation of the width at small values of L that flattens around $L = 48$. In the present paper we do not attempt to quantitatively describe the finite volume artefacts. This issue forms the subject of a separate investigation and we plan to address it in the future.

From Fig. 5 it is also seen that the effect of the background on the real part of the pole position is small, whereas the imaginary part is far more sensitive to it. Namely, the two values of E_0, calculated at $L = 60$ for $k_{\mathsf{max}} = 0$ and $k_{\mathsf{max}} = 10$ differ by $\simeq 0.2\%$, whereas the same calculation for the width yields $\Gamma_\eta = (0.91 \pm 0.04) \cdot 10^{-2}$ and $\Gamma_\eta = (1.17 \pm 0.05) \cdot 10^{-2}$, respectively. In general, one may conclude that the effect of the background can not be neglected.

The final result for the real and imaginary parts of the pole position (for $L = 60$) are

$$
\begin{aligned}
m_\eta &= 2m_\phi + E_0 = 0.5074 \pm 0.0004\,, \\
\Gamma_\eta &= \Gamma = (1.17 \pm 0.05) \cdot 10^{-2}
\end{aligned}
\tag{32}
$$

(errors are only statistical). This result can be checked by using the effective-range expansion for the scattering phase (cf. with Ref. [27])

$$
-\frac{p}{W}\tan\delta(p) = a - bp^2\,, \qquad W = 2\sqrt{m_\phi^2 + p^2}\,,
\tag{33}
$$

where the parameters a and b are related to m_η and Γ_η through

$$
m_\eta = 2\sqrt{m_\phi^2 + \frac{a}{b}}\,, \qquad \Gamma_\eta = \frac{4}{bm_\eta^2}\sqrt{\frac{a}{b}}\,.
\tag{34}
$$

As one sees from Fig. 6, our phase shift results are generally in agreement with the results of the Ref. [27]. However, since the data are not *exactly* linear, the question arises, which
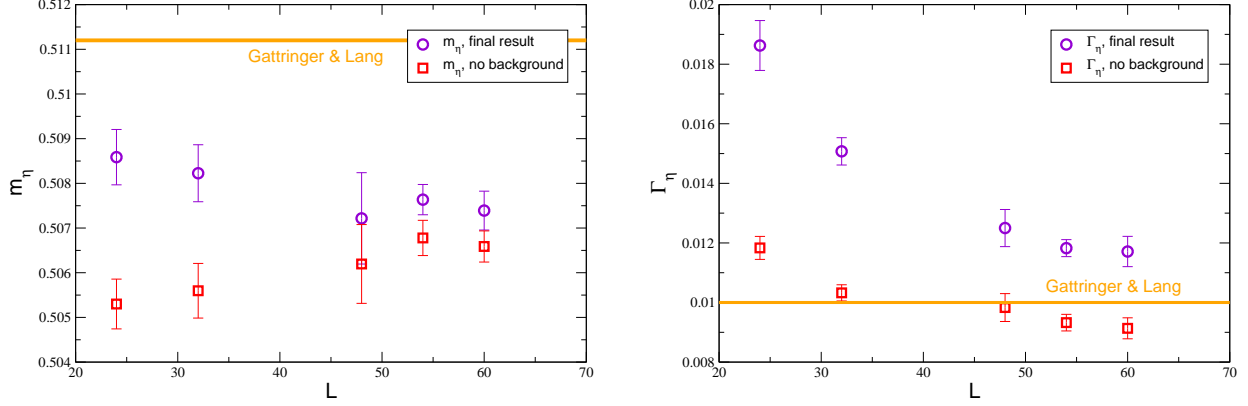
14

FIG. 5: The energy and the width of the resonance, extracted from the data at $k_{\mathsf{max}} = 10$ (final result). For comparison, we display the result at $k_{\mathsf{max}} = 0$ (no background) and the result, taken from Refs. [27, 28] (the error quoted in these references corresponds to the thickness of the lines). The errors in our calculations are purely statistical.

interval in the variable p^2 should be used in the fit to determine the coefficients a and b. For instance, the extracted values of the phase shift *in the vicinity of the resonance* $(p/m_\phi)^2 \simeq 0.8$ neatly follow the straight line with the parameters a, b, which were determined from Eqs. (33), using the central values of m_η, Γ_η in Eq. (32).

Now, we are in a position to compare our results to those of Refs. [27, 28]. The difference in the real part of the resonance pole position is small – both results agree with an accuracy of better than one per cent. The effect is larger in the imaginary part. However, one should keep in mind that the magnitude of the imaginary part is approximately 50 times smaller than the real part. As one concludes from Fig. 6, a relatively large effect in the imaginary part could be related, e.g., to the fact that the effective range plot is not exactly linear. Therefore, it seems plausible that the systematic errors both in Refs. [27, 28] and in the present paper are underestimated. We expect that the results should agree within the errors.

Comparing our method to Lüscher's approach, we further note that, once the plateau in L sets in, the energy and the width within our method can be extracted at *a single* value of L. In contrast to this, Lüscher's approach implies the study of the volume dependence of the energy levels. This difference can be related to the fact that our method uses additional input information from MC simulations. In particular, apart from the energy spectrum, the two-point function $C_{11}(t)$ contains the information about the transition matrix elements encoded in the constants $z_l, \ l \neq 1$.

Last but not least, we have also checked that our method works in the non-interacting case as well. Setting $g = 0$ and adjusting κ_ϕ, κ_η in the Lagrangian to keep the masses of ϕ and η the same as in the interacting case (see Refs. [27, 28]), we have done the calculation of the function $C_{11}(t)$ anew. The fitted width turns out to be two orders of magnitude smaller as compared to the interacting case. This obviously corresponds to a stable particle.
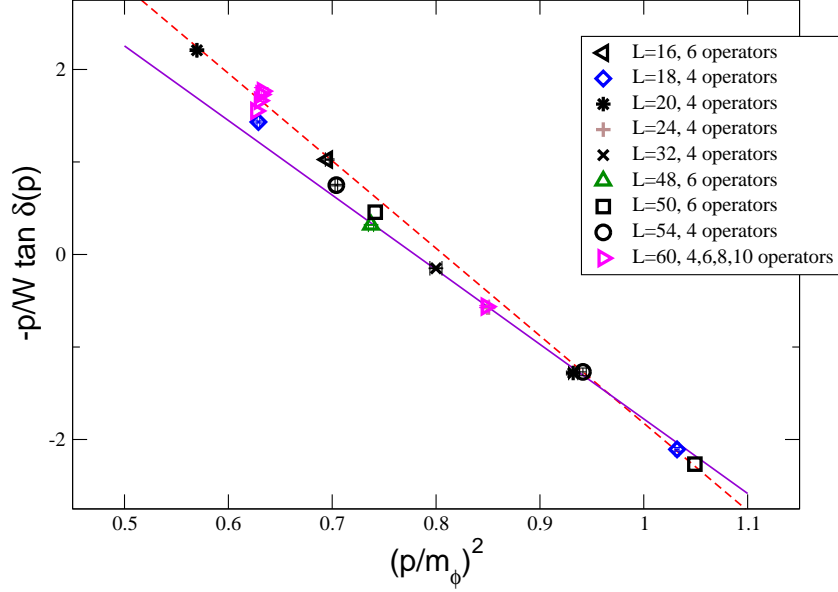
FIG. 6: The quantity $-p/W \tan \delta(p)$, extracted from the energy spectrum, vs. $(p/m_\phi)^2$. The solid line is the linear fit $a - bp^2$, with a, b determined from Eqs. (32) and (34), using the central values of m_η and Γ_η. To draw the dashed line, we have used m_η, Γ_η from Ref. [27] instead of Eq. (32) (cf. with Fig. 2 of that paper). The errors in the data are purely statistical. In addition, we have indicated the dimension of the operator basis O_j used to extract the spectrum.

VII. CONCLUSIONS

i) In the present paper we have proposed a novel method to extract the resonance pole position on the lattice. The method is based on the universal representation of the two-point function Eq. (20), which is valid given the sole assumption that an isolated low-lying resonance is present in the system. The energy and the width of this resonance are determined from the fit of Eq. (20) to the lattice MC data. It remains to be seen whether such a universal representation can be derived in more complicated cases (e.g., for the multi-channel scattering, see Ref. [38]) as well.

ii) The proposed method provides an alternative to Lüscher's approach to the resonances. In the latter, the *volume dependence* of the *spectrum* on the moderately large lattices is studied. The spectrum consists of the scattering states only – the resonance has already decayed. In our approach the two-point function is studied *at finite times t* (when the resonance is still "alive") and for the *asymptotically large* values of L. Note that the actual calculations do not seem to require extraordinarily large volumes. For example, in the 1+1 dimensional Ising model $L = 48$ was already sufficient.

iii) The above difference entails an important advantage of the method described in this paper: whereas in Lüscher's approach the MC simulations should be performed at least at several volumes in order to extract the resonance, the measurement at one, albeit sufficiently large, lattice volume suffices in our method.

iv) In certain cases, the numerical accuracy of the method can be improved considerably, if the multi-exponential representation of the two-point function is used in the fit

16

instead of calculating this function directly through MC simulations at all values of t. The coefficients of the multi-exponential representation are obtained by solving the generalized eigenvalue problem and, in particular, encode the decay matrix elements.

v) Recently, the excited meson and baryon spectra have been determined by several lattice collaborations using the generalized eigenvalue equation (see, e.g. Refs. [19–21] for the latest work on the subject). These calculations closely resemble the calculations in the 1+1 dimensional toy model, which were presented in this paper. In our opinion, it would be very interesting to apply the proposed method to the data and if possible try to locate the resonance pole(s). This can be done at *no additional cost,* since the results of already existing MC simulations would be used.

Acknowledgments

Appendix A: Continuum limit in the matrix elements

The regular summation theorem [29], which is used in order to perform the continuum limit in the sums over the discrete momentum eigenvalues, implies that the integrand is a continuous function in the momenta. However, the finite-volume matrix elements $\langle 0|\phi(0)|\beta\rangle$, which enter Eq. (8), contain Lüscher's zeta-function and can become singular. Here, for one particular example, we shall demonstrate how these singularities are lifted.

The averaged quantities, for which the validity of the regular summation theorem will be checked, are defined in Eq. (11). From now on, without loss of generality, we shall work in the center-of-mass frame $\mathbf{k} = 0$. We wish to demonstrate that

$$\lim_{L\to\infty} A(\omega_0, \Delta, \mathbf{0}) = A^\infty(\omega_0, \Delta, \mathbf{0}), \qquad \omega_0 > \omega_{\mathsf{min}}, \quad \Delta > 0. \tag{A1}$$

More precisely, the difference between the both sides of the above equation vanishes faster that any negative power of L, as $L \to \infty$.

Let ω_0 be in the elastic scattering region. Since L is large, characteristic momenta are small and non-relativistic quantum mechanics provides an adequate description of a problem under consideration. Let us consider two massive (distinguishable) particles in the CM frame. The state vector corresponding to the eigenvalue E_β is given by

$$|\beta\rangle = \frac{1}{L^{d/2}} \sum_{\mathbf{q}} f_\beta(\mathbf{q}) \,|\mathbf{q}, -\mathbf{q}\rangle, \qquad |\mathbf{q}, -\mathbf{q}\rangle = a_1^\dagger(\mathbf{q}) a_2^\dagger(-\mathbf{q})|0\rangle, \tag{A2}$$

where $a_i^\dagger$, $i = 1, 2$ denote the creation operators for the particles 1 and 2, respectively, and the wave function $f_\beta(\mathbf{q})$ is normalized, according to

$$\langle\beta|\beta\rangle = \frac{1}{L^d} \sum_{\mathbf{q}} |f_\beta(\mathbf{q})|^2 = 1. \tag{A3}$$

For simplicity, let us further assume that the interaction between the particles is described by a separable potential $V(\mathbf{p}, \mathbf{k}) = g v(\mathbf{p}) v(\mathbf{k})$, where the function $v(\mathbf{p})$ corresponds to a smooth cutoff at large momenta. Note that in the following we will never need the explicit form of this function. The T-matrix is given by

$$T(\mathbf{p}, \mathbf{q}; E) = \frac{v(\mathbf{p}) v(\mathbf{q})}{g^{-1} - I(E)}, \qquad I(E) = \frac{1}{L^d} \sum_{\mathbf{k}} \frac{v^2(\mathbf{k})}{\mathbf{k}^2 - k_0^2}, \qquad k_0^2 = 2\mu E, \qquad (A4)$$

where μ denotes the reduced mass of the system.

In the limit $E \to E_\beta$ the T-matrix has a pole. In the vicinity of the pole, it behaves as

$$T(\mathbf{p}, \mathbf{q}; E) = \frac{v(\mathbf{p}) v(\mathbf{q})}{g^{-1} - I(E_\beta) - I'(E_\beta)(E - E_\beta) + \cdots} = \frac{v(\mathbf{p}) v(\mathbf{q})}{-I'(E_\beta)(E - E_\beta) + \cdots}. \qquad (A5)$$

From this expression, we may read off the wave function corresponding to the eigenvalue E_β

$$f_\beta(\mathbf{q}) = \sqrt{\frac{2\mu}{I'(E_\beta)}} \frac{v(\mathbf{q})}{\mathbf{q}^2 - k_{0\beta}^2}, \qquad k_{0\beta}^2 = 2\mu E_\beta. \qquad (A6)$$

The normalization of this wave function was chosen so that $f_\beta(\mathbf{p})$ obeys Eq. (A3).

Take the composite field $\phi(0) = \phi_1(0)\phi_2(0)$, where the $\phi_i(0)$, $i = 1, 2$ denote the elementary particle fields. In momentum space,

$$\phi_i(0, \mathbf{x}) = \frac{1}{L^{d/2}} \sum_{\mathbf{k}} e^{i\mathbf{k}\mathbf{x}} a_i(\mathbf{k}) \qquad (A7)$$

The matrix element that enters the spectral function is given by

$$\langle 0 | \phi(0) | \beta \rangle = \frac{1}{L^{3d/2}} \sum_{\mathbf{q}} f_\beta(\mathbf{q}) \doteq \frac{1}{L^d} \tilde{f}_\beta(\mathbf{0}), \qquad (A8)$$

where $\tilde{f}_\beta(\mathbf{r})$ denotes the Fourier-transform of $f_\beta(\mathbf{q})$. The averaged spectral function is written in the following form

$$A(\omega_0, \Delta, \mathbf{0}) = \frac{1}{L^d} \sum_{\beta} \theta(\omega_0 + \Delta/2 - E_\beta)\theta(E_\beta - \omega_0 + \Delta/2) \, |\tilde{f}_\beta(\mathbf{0})|^2. \qquad (A9)$$

Hence, in order to verify the applicability of the regular summation theorem in this case, it suffices to show that $\tilde{f}_\beta(\mathbf{0})$ is a regular function of $k_{0\beta}$. As anticipated, this function contains Lüscher's zeta-function which is singular at $k_{0\beta}^2 = (2\pi\mathbf{n})^2/L^2$. However, the factor $I'(E_\beta)$, which enters the normalization, contains the zeta-function as well. It is easy to check that the singular factors in the numerator and the denominator cancel, and the regular summation theorem holds.

Appendix B: Emergence of the second Riemann sheet in the infinite volume limit

Let us consider[6] the function F_L of the complex variable z

$$F_L(z) = \frac{1}{1 - z + \epsilon^2 \sqrt{z} \cot(\sqrt{z}L)}, \qquad z \in \mathbb{C}. \qquad (B1)$$

---

[6] We are indebted to Jürg Gasser who indicated this example to us.

Note that this function resembles the propagator of an unstable particle in the 1+1-dimensional effective field theory [5]. Further, it can be shown that

$$\text{sign}(\text{Im}\,(\sqrt{z}\cot(\sqrt{z}L))) = -\text{sign}(\text{Im}\,(z))\,. \tag{B2}$$

According to this condition, the denominator can not vanish outside the real axis. Thus, the only singularities of $F_L(z)$ are simple poles on the positive real axis.

If $\text{Im}\,(z) \neq 0$, in the limit $L \to \infty$ we have $\cot(\sqrt{z}L) \to -i\,\text{sign}(\text{Im}\,(z))$ and, therefore,

$$F_\infty(z) = \frac{1}{1 - z + \epsilon^2\sqrt{-z}}\,. \tag{B3}$$

The difference $|F_L(z) - F_\infty(z)|$ vanishes exponentially with L, if $\text{Im}\,(z) \neq 0$. Note that, unlike $F_L(z)$, which is a meromorphic function, $F_\infty(z)$ is analytic in the complex plane cut along the positive real axis. This is what is meant when we speak of "the poles merging into the cut".

Moreover, the function $F_\infty(z)$ has a couple of complex-conjugated poles *on the second Riemann sheet*. These poles are solutions of the equation $1 - z + \epsilon^2\sqrt{-z}$ that gives $z_\pm = 1 \mp i\epsilon^2 + O(\epsilon^4)$. If ϵ^2 is small, these poles come close to the physical scattering region and influence $F_\infty(z)$ on the physical sheet. Since away from the real axis the difference between $F_\infty(z)$ and $F_L(z)$ vanishes exponentially at a large L, the effect of the poles on the second Riemann sheet is felt in $F_L(z)$ as well.

---

[1] M. Lüscher, DESY-88-156 *Lectures given at Summer School 'Fields, Strings and Critical Phenomena', Les Houches, France, Jun 28 - Aug 5, 1988*;

[2] U.-J. Wiese, Nucl. Phys. Proc. Suppl. **9** (1989) 609;

[3] M. Lüscher, Nucl. Phys. B **354** (1991) 531.

[4] M. Lüscher, Nucl. Phys. B **364** (1991) 237.

[5] D. Hoja, U.-G. Meißner and A. Rusetsky, arXiv:1001.1641 [hep-lat].

[6] M. Göckeler, H. A. Kastrup, J. Westphalen and F. Zimmermann, Nucl. Phys. B **425** (1994) 413 [arXiv:hep-lat/9402011].

[7] S. Aoki *et al.* [CP-PACS Collaboration], Phys. Rev. D **76** (2007) 094506 [arXiv:0708.3705 [hep-lat]].

[8] M. Göckeler, R. Horsley, Y. Nakamura, D. Pleiter, P. E. L. Rakow, G. Schierholz and J. Zanotti [QCDSF Collaboration], PoS **LATTICE2008** (2008) 136 [arXiv:0810.5337 [hep-lat]].

[9] K. Rummukainen and S. A. Gottlieb, Nucl. Phys. B **450** (1995) 397 [arXiv:hep-lat/9503028].

[10] M. Asakawa, T . Hatsuda and Y . Nakahara, [arXiv:hep-lat/0011040v2]

[11] S. Sasaki, K. Sasaki, T. Hatsuda and M. Asakawa, Nucl. Phys. Proc. Suppl. **119** (2003) 302 [arXiv:hep-lat/0209059].

[12] K. Sasaki, S. Sasaki and T. Hatsuda, Phys. Lett. B **623** (2005) 208 [arXiv:hep-lat/0504020].

[13] C. Michael, Nucl. Phys. B **327** (1989) 515.

[14] R. D. Loft and T. A. DeGrand, Phys. Rev. D **39** (1989) 2692.

[15] L. Lellouch and M. Lüscher, Commun. Math. Phys. **219** (2001) 31 [arXiv:hep-lat/0003023].

[16] J. J. Dudek, R. G. Edwards, M. J. Peardon, D. G. Richards and C. E. Thomas, Phys. Rev. Lett. **103** (2009) 262001 [arXiv:0909.0200 [hep-ph]].

[17] S. Cohen *et al.*, arXiv:0911.3373 [hep-lat].

[18] J. M. Bulava *et al.*, Phys. Rev. D **79** (2009) 034505 [arXiv:0901.0027 [hep-lat]].

[19] J. Bulava *et al.*, arXiv:1004.5072 [hep-lat].

[20] J. J. Dudek, R. G. Edwards, M. J. Peardon, D. G. Richards and C. E. Thomas, arXiv:1004.4930 [hep-ph].

[21] G. P. Engel, C. B. Lang, M. Limmer, D. Mohler and A. Schafer [BGR [Bern- Graz-Regensburg] Collaboration], arXiv:1005.1748 [hep-lat].

[22] A. Walker-Loud *et al.*, Phys. Rev. D **79** (2009) 054502 [arXiv:0806.4549 [hep-lat]].

[23] T. Burch, C. Gattringer, L. Y. Glozman, C. Hagen, D. Hierl, C. B. Lang and A. Schafer, Phys. Rev. D **74** (2006) 014504 [arXiv:hep-lat/0604019].

[24] C. Alexandrou and A. Tsapalis, Phys. Rev. D **73** (2006) 014507 [arXiv:hep-lat/0503013].

[25] C. Alexandrou and A. Tsapalis, PoS **LAT2005** (2006) 023 [arXiv:hep-lat/0509139].

[26] Z. Y. Niu, M. Gong, C. Liu and Y. Shen, Phys. Rev. D **80** (2009) 114509 [arXiv:0909.3154 [hep-lat]].

[27] C. R. Gattringer and C. B. Lang, Phys. Lett. B **274** (1992) 92

[28] C. R. Gattringer and C. B. Lang, Nucl. Phys. B **391** (1993) 463 [arXiv:hep-lat/9206004].

[29] M. Luscher, Commun. Math. Phys. **105** (1986) 153.

[30] B. S. DeWitt, Phys. Rev. **103** (1956) 1565.

[31] A. Nolan, M. Peardon and A. O Cais, PoS **LAT2007** (2007) 127.

[32] T. R. Hemmert, B. R. Holstein and J. Kambor, J. Phys. G **24** (1998) 1831 [arXiv:hep-ph/9712496].

[33] V. Bernard, U.-G. Meißner and A. Rusetsky, Nucl. Phys. B **788** (2008) 1 [arXiv:hep-lat/0702012].

[34] V. Bernard, D. Hoja, U.-G. Meißner and A. Rusetsky, JHEP **0906** (2009) 061 [arXiv:0902.2346 [hep-lat]].

[35] H. Krebs, E. Epelbaum and U.-G. Meißner, Phys. Lett. B **683**, 222 (2010) [arXiv:0905.2744 [hep-th]].

[36] M. R. Schindler and D. R. Phillips, Annals Phys. **324** (2009) 682 [Erratum-ibid. **324** (2009) 2051] [arXiv:hep-ph/0808.3643].

[37] R. H. Swendsen and J. -S. Wang, Phys. Rev. Lett. **58** (1987) 86

[38] M. Lage, U.-G. Meißner and A. Rusetsky, Phys. Lett. B **681**, 439 (2009) [arXiv:0905.0069 [hep-lat]].